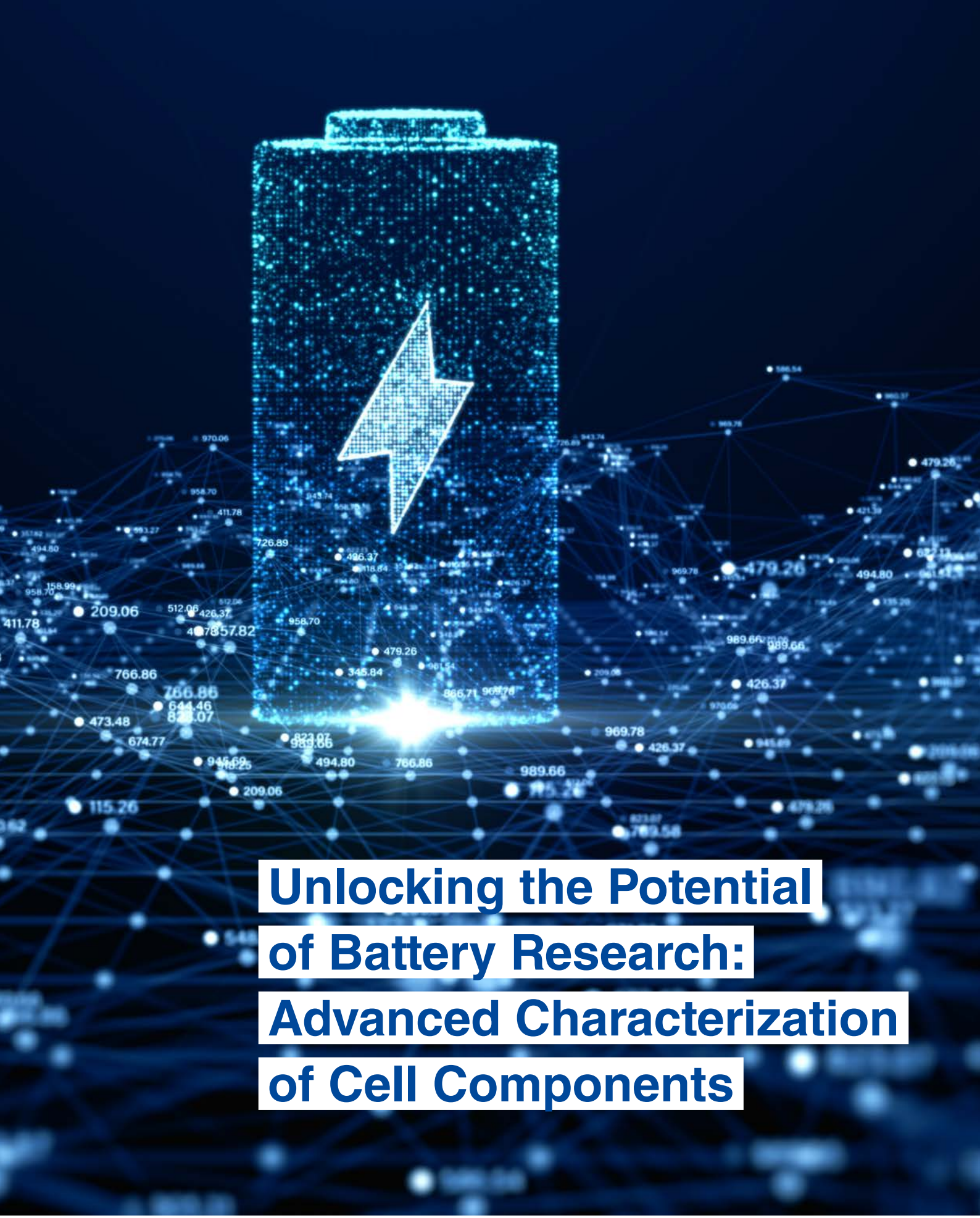

Unlocking the Potential of Battery Research: Advanced Characterization of Cell Components

PerkinElmer®
For the Better

Wiley Analytical Science

Imprint

Boschstr. 12, 69469 Weinheim, Germany

Email: info@wiley-vch.de
Editors: Dr. Martin Graf-Utzmann & Róisín Murtagh
Ad Sales: Bettina Willnow

Cover image © AdobeStock | KanawatTH

Contents

Introduction

Battery research has become increasingly important in recent years due to the growing demand for reliable, efficient, and cost-effective energy storage solutions. Advanced battery research is focused on improving the performance, safety, and lifespan of batteries, as well as reducing their environmental impact.

Advanced characterization of cell components for battery producers is a key area of research. This involves studying the physical and chemical properties of individual components such as electrodes, separators, and electrolytes. Understanding these components better can help manufacturers optimize the design and performance of their batteries.

Battery recycling is another critical area of research. This involves finding ways to reuse and re-manufacture used batteries to extend their life and reduce the strain on landfill sites. Researchers are developing new technologies to identify and extract valuable materials from used batteries and to repurpose them for use in new batteries.

Finally, energy storage research is focused on finding ways to store energy efficiently and safely. This includes studying the properties of different materials and chemistries to find new and improved ways of storing energy. Researchers are also exploring the use of advanced technologies such as flow batteries and supercapacitors to extend the lifespan and improve the performance of energy storage systems.

This expert insight begins with a study by Barbosa *et al.* (2022) on three-component solid polymer electrolytes based on Li-ion exchanged microporous silicates and an ionic liquid for solid-state batteries. The article discusses the use of solid polymer electrolytes (SPEs) as a way to overcome toxicity and degradation issues associated with Li-ion batteries (LIBs) in the digital age. SPEs can be tuned with a host polymer matrix and optimized with the balance between different matching fillers, such as Li salts, ionic liquids (ILs), ceramic materials, and metal-organic frameworks. Their work focuses on developing high-performance SPEs with a combination of different zeolite structures with and without the ion exchange capability and IL[BMIM][SCN] as a complementary filler trapped within a polar PVDF-HFP polymer matrix. The combination of microporous silicates and ILs are used to improve their individual properties and enhance the overall performance stability of the SPE.

Next, Chen *et al.* (2022) discuss various methods of recycling LIBs, with a particular focus on the flash recycling method (FRM). FRM involves selective heating of the resistive layer by ultrafast electrothermal reactions to dissolve the SEI, polymer binder, and intercalated molecules, along with the formation of a close-contact carbon coating while maintaining the graphite particle morphology. Further, dilute acid treatment is used to recover other decomposition products (LiF, Li_2O, CoO, etc.). The flash-recycled anode is found to show better rate performance and electrochemical stability when compared to untreated AW and calcination-recycled anode. A life-cycle assessment of all available methods is also discussed.

Finally, Tanim *et al.* (2022) investigate the less-researched area of cathode degradation issues during XFC of electric vehicles, especially for low Ni-containing MNCs like graphite/NMC532 single-layer pouch cells. It is found to be more severe under moderate loading and aging for NMC532 becomes dominant in later cycles. The cracking of inter-primary particles and surface reconstruction are the main causes of degradation. NMC811, a low Co-content cathode candidate, is chosen for its potential in high-energy-density

Li-ion battery applications. A wide-ranging study is conducted to explore its performance at different fast charging rates and SOCs. SEM-EBSD and two different modeling tools are used to predict NMC811's performance and aging in comparison to NMC532.

Overall, battery research is an important and rapidly evolving field. Advances in battery research are essential for meeting the growing demand for reliable and efficient energy storage solutions. By improving the performance, safety, and lifespan of batteries, as well as reducing their environmental impact, battery research is playing an essential role in the development of a sustainable energy future.

Through the methods and applications presented in this expert insight, we hope to educate researchers on new technologies and techniques in battery research. For more information, we encourage you to visit PerkinElmer to learn more and explore options to enhance your research.

Róisín Murtagh
Editor at Wiley Analytical Science

References

Barbosa, J.C., Correia, D.M., Salado, M., Gonçalves, R., Ferdov, S., de Zea Bermudez, V., Costa, C.M. and Lanceros-Mendez, S. (2023), Three-Component Solid Polymer Electrolytes Based on Li-Ion Exchanged Microporous Silicates and an Ionic Liquid for Solid-State Batteries. Adv. Eng. Mater., 25: 2200849. https://doi.org/10.1002/adem.202200849

Chen, W., Salvatierra, R. V., Li, J. T., Kittrell, C., Beckham, J. L., Wyss, K. M., La, N., Savas, P. E., Ge, C., Advincula, P. A., Scotland, P., Eddy, L., Deng, B., Yuan, Z., Tour, J. M., Flash Recycling of Graphite Anodes. Adv. Mater. 2023, 35, 2207303. https://doi.org/10.1002/adma.202207303

Tanim, T. R., Yang, Z., Finegan, D. P., Chinnam, P. R., Lin, Y., Weddle, P. J., Bloom, I., Colclasure, A. M., Dufek, E. J., Wen, J., Tsai, Y., Evans, M. C., Smith, K., Allen, J. M., Dickerson, C. C., Quinn, A. H., Dunlop, A. R., Trask, S. E., Jansen, A. N., A Comprehensive Understanding of the Aging Effects of Extreme Fast Charging on High Ni NMC Cathode. Adv. Energy Mater. 2022, 12, 2103712. https://doi.org/10.1002/aenm.202103712

Three-Component Solid Polymer Electrolytes Based on Li-Ion Exchanged Microporous Silicates and an Ionic Liquid for Solid-State Batteries

Adapted from Barbosa *et al.* (2022)

The age of digitalization massively increases the application of Li-ion batteries (LIB) instead of having rising concerns about toxicity and degradation issues related to liquid electrolytes. Solid polymer electrolytes (SPEs) can overcome these issues by tuning their properties with a host polymer matrix and optimizing the balance between different matching fillers, such as Li salts, ionic liquids (ILs), ceramic materials, and metal-organic frameworks (MOFs). A combination of ILs and MOFs particularly enhances the structural stabilization of SPEs. Replacing MOFs with zeolites turns out to be an eco-friendlier solution in terms of delivering high ionic conductivity and stabilized battery performance. This work focuses on developing high-performance SPEs with a combination of different zeolite structures with and without the ion exchange (IE) capability and IL[BMIM][SCN] as a complementary filler trapped within a polar PVDF-HFP polymer matrix. Combining these complementary fillers, i.e., microporous silicates and ILs, to improve their individual properties and therefore enhance the overall performance stability of the SPE is the novelty of this work.

The IE process was carried out in an aqueous solution of 1M LiOH, which was added at a rate of 50 mL to each 0.5g zeolite powder sample. The solution was treated in a furnace at 90°C for 72 hours and then filtered accordingly. The doctor blade technique was used to prepare three composite SPE samples (with 60:40 polymer: IL ratio and 84:16 polymer: zeolite ratio) and their equivalent IE counterparts with natural zeolite clinoptilolite (CPT), synthetic microporous titanosilicates ETS-4 and ETS-10 structures. The same procedure was used to prepare a reference PVDF-HFP sample with 40wt.% of [BMIM][SCN] inclusion for comparison purposes. The microstructural, thermal, mechanical, and electrochemical properties of these samples were thoroughly characterized to understand their performance stability.

Figure 1 shows the HRTEM images of these tri-composite samples (containing polymer, IL, and zeolite) having a homogeneous and almost compact structure (except the presence of voids at the surface level, which positively contributes towards the battery performance) irrespective of the zeolite type and IE capability. Varying Li-content of these tri-compos-

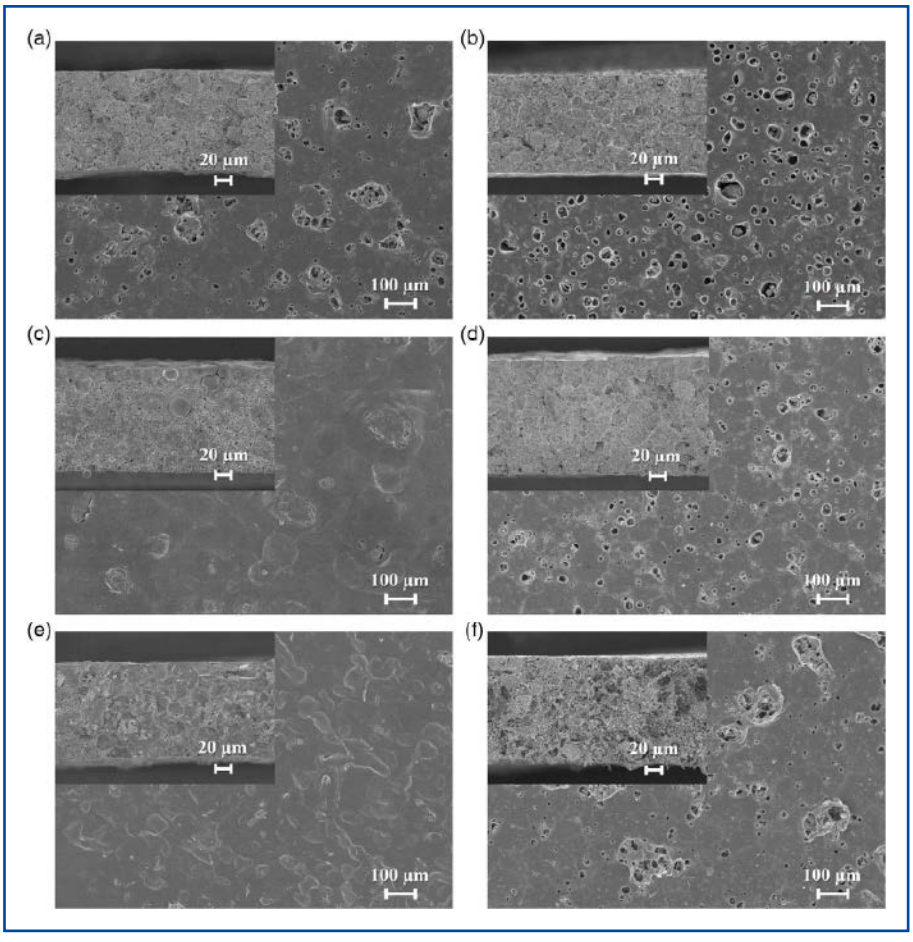

Figure 1. Surface and cross-section scanning electron microscope (SEM) images of: a) natural zeolite clinoptilolite (CPT), b) CPT IE, c) ETS-4, d) ETS-4 IE, e) ETS-10 , f) ETS-10 IE.

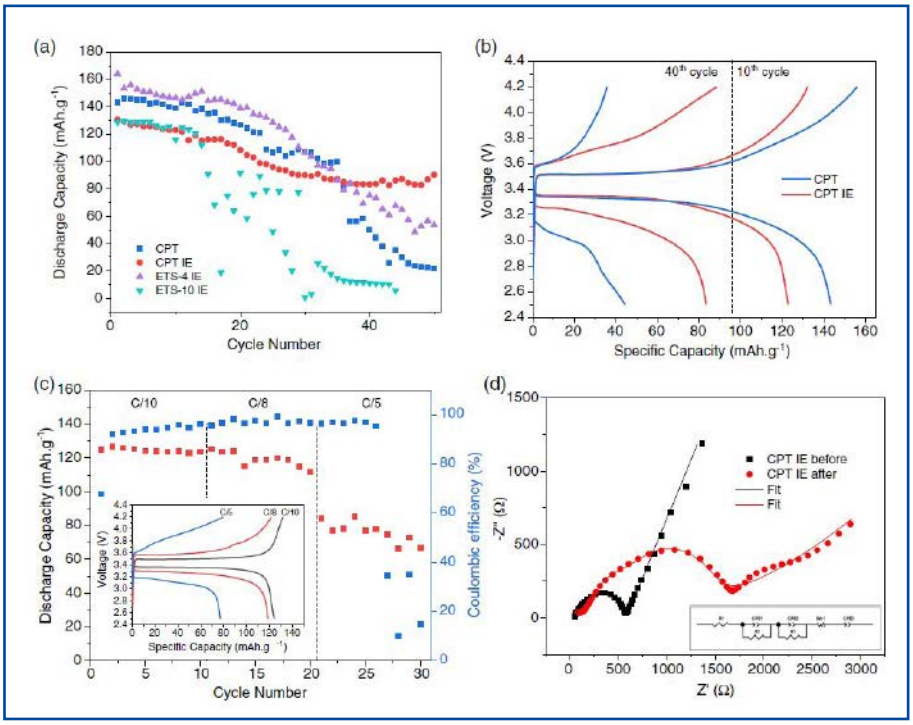

Figure 2. a) Cycling stability of the different solid polymer electrolytes (SPEs) at C/10; b) comparison between the charge/discharge profiles at the 10th and 40th cycles for the CPT and CPT IE samples; c) cycling performance of the CPT IE sample at different discharge rates at room temperature and respective charge/discharge profiles at the 5th cycle of each rate; d) impedance spectroscopy of the CPT IE sample before and after cycling (Inset: fitting of the equivalent circuit).

ite samples leads to different electrostatic interactions and, therefore, different ionic conductivity values. On the other hand, XRD patterns reveal that the higher Li-concentration typically leads to lower crystallinity as compared to their Li-free counterparts, and different filler types also affect the crystallinity; for example, ETS-10 has the highest crystallinity (48%) followed by PVDF-HFP (35 – 37%), ETS-4 (33%), and CPT (31%). The FTIR/ATR spectra confirm that all samples contain >85% β-phase due to the [BMIM][SCN] inclusion in their structure, except neat PVDF-HFP.

The thermal behavior analyzed in a Perkin–Elmer DSC 6000 equipment shows polymer melting for the neat PVDF-HFP sample and destabilized crystalline phases in the tri-composite samples because of their ion-dipole electrostatic interaction between IL[BMIM][SCN] and polar polymer chains. This is further supported by the TGA analysis, where composite samples show several weight-loss steps due to different degradation phenomena (water evaporation, degradation of IL and microporous solid, etc.), and the neat PVDF-HFP sample shows a single weight-loss step confirming polymer melting. This also leads to the lower mechanical stability of composite samples due to IL[BMIM][SCN]'s plasticity effect and reinforcement of polymer matrix via zeolite structure when compared to the neat PVDF- HFP sample. Particularly, IE improves the mechanical properties of CPT and ETS-4 but reduces the same for ETS-10. Although the tri-composite samples show Young's modulus of up to 98 MPa and thermal stability of up to 100°C irrespective of their zeolite structure and IE processes, they are still found suitable for LIB-SPE applications.

The ionic conductivity has been evaluated by Electrochemical Impedance Spectroscopy. The Nyquist plots reveal the characteristic ion diffusion process via the presence of mobile charge carriers. The Arrhenius plots show a decrease in the resistance with increasing temperature because of BMIM][SCN] dissociation leading to abundant free charges and higher mobility of the polymer chains, therefore supporting the ionic conductivity. Although the ionic conductivity is primarily dependent on IL and can be increased upon IE, the incorporation of zeolites can also reduce that. The degree of crystallinity, different pore systems, size, and amount of water molecules in the zeolites lead to the highest ionic conductivity in CPT followed by ETS-4 and ETS-10. In addition, all these samples show excellent electrochemical stability between 0-4.5V reference window

at ambient conditions indicating their suitability for LIB application.

The performance and life cycle tests for tri-composite samples are performed with and without IE at room temperature for 50 cycles are shown in **Figure 2**. CPT has a higher initial discharge capacity of 140 mAh/g, but a significant loss is noted due to structural destabilization after 40 cycles. CPT-IE displays the most stable behavior among all the samples with an initial discharge capacity of about 130 mAh/g followed by a 30% decrease after 50 cycles. CPT-IE also shows no capacity loss at C/10 and C/8 rates, and a high Coulombic efficiency (up to 95%) except in the first cycle, where the system is still in activation mode. During cycling, the formation of a solid electrolyte interface layer significantly increases the overall resistance (from 600 to 1700 Ω) of CPT samples as revealed by the Nyquist plot. Thus, IE offers improved discharge capacity, a very good rate performance, and stabilization of the SPE structure irrespective of the cycles indicating it as a promising technology for LIB application.

The results obtained from this work have addressed the largely reported high-temperature issues associated with the battery application. The benefits of this two-filler approach are improved cyclic stabilization of the SPE structure and high performance, which are obtained by the addition of microporous silicates and IL. The addition of zeolite structures increases the number of Li ions, which are responsible for better conductivity in a battery. Moreover, the zeolites also improve the thermal and mechanical stability of the SPE structure as compared to their counterparts when prepared using only IL (i.e., no zeolites). An overall enhancement of the battery performance is observed when the IE process is employed indicating their potential for the next-generation solid-state LIB application.

Digest of
Barbosa J, Correia D, Salado M, et al. Three-Component Solid Polymer Electrolytes Based on Li-Ion Exchanged Microporous Silicates and an Ionic Liquid for Solid-State Batteries. Adv. Eng. Mater., 25: 2200849.

Flash Recycling of Graphite Anodes

Adapted from Chen *et al.* (2022)

Commercial recycling of Li-ion batteries mostly focuses on the retrieval of valuable materials (Li, Co, Ni, and Mn) from the cathodes, whereas low-cost graphite anodes are left for either sourcing energy or landfilling. Although anode recycling has received less attention from the industry, several methods, including a Fenton reagent-assisted flotation process, hydrometallurgical methods followed by filtration, a combined sulfuric acid curing, leaching and high-temperature calcination process, and a multistep heating and sintering process have been investigated on the laboratory-scale. However, acid contamination of graphite, high-temperature heating cost, left-over organic and inorganic impurities, and noticeable performance gap between pristine and regenerated anodes have limited the commercial application of these methods. Particularly, the insoluble Li organic and inorganic salts form a complex insulating layer on the anode affecting its performance but preventing detrimental erosion. Thus, it is worth recycling the passivated graphite anode if its pristine structure is preserved underneath. This work describes the flash recycling method (FRM), which directly treats the anode waste (AW) by a flash Joule heating (FJH) process followed by a dilute acid (0.1M HCl) treatment while recovering the valuable battery-metal resources. FRM involves selective heating of the resistive layer by ultrafast electrothermal reactions according to Joule's law. The high pulse current leads to the dissociation of SEI, polymer binder, and intercalated molecules, along with the formation of a close-contact carbon coating while maintaining the graphite particle morphology. In addition, other decomposition products (LiF, Li_2O, CoO, etc.) are recovered by the dilute acid treatment. The flash-recycled anode (FRA) shows better rate performance and electrochemical stability when compared to untreated AW and calcination-recycled anode (CRA). The electrochemical stability and rate performance of FRA in comparison with others are also validated for fuel cells with $LiFePO_4$ cathode, followed by an LCA of all available methods.

Figure 1 schematically represents the FRM for the graphite anode. The powdered graphite AW collected from the spent batteries is less resistive than the SEI layer and other impurities, thus selective electrothermal effect can be achieved in ~1s via capacitor banks in the FJH circuit. A FEM simulation indicates the flash temperature is rapidly dissipated to the surroundings preventing any thermal expansion and defect formation in the anode leading to the homogeneous temperature distribution. The high pulse current and ultrafast heating rate lead to the thermal decomposition of typical hard-to-dissolve compact solid electrolyte interphases and binders and the formation of simple inorganic salts, metal oxide nanoparti-

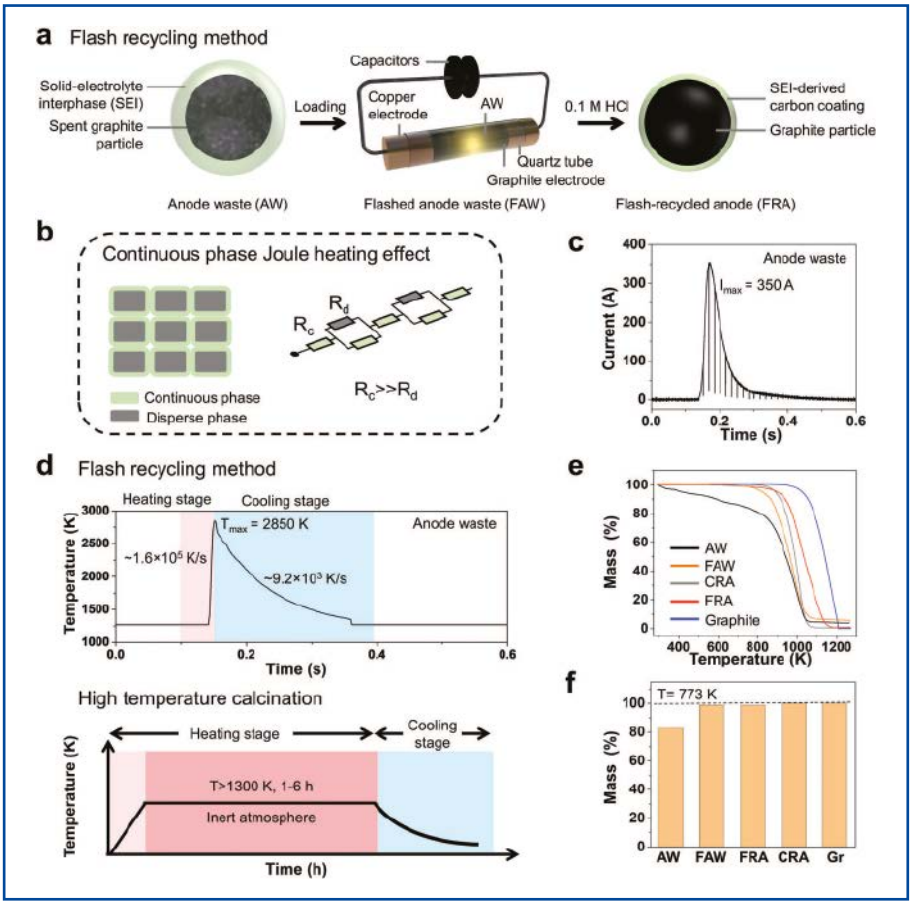

Figure 1. Flash recycling of graphite anodes. Schematic of a) flash recycling of AW and b) resistance-dependent Joule heating effects in multiple phase systems. c) Corresponding current-time curve during the flash recycling process. d) General procedures for flash recycling compared with conventional high temperature calcination and their real-time temperature curves. e) TGA thermogram of different graphite anodes. f) The remaining mass ratios of different graphite anodes at T = 773 K compared to the initial mass at 298 K. AW: anode waste. FAW: flashed anode waste. FRA: flash-recycled anode. CRA: calcination-recycled anode. Gr: graphite.

cles, and a close-contact carbon coating with embedded nanoparticles. This thermal decomposition is evidenced by TGA analysis, where ~17.3% and ~1.4% mass loss at 773K for untreated AW and FRA, respectively, are observed, indicating the latter has more graphitic stability. CRA shows ~0.1% mass loss at 773K due to the direct evaporation of transition metals at high temperatures. However, the temperature at which 50% mass loss takes place for FRA is ~90K and ~50K higher than that of AW and CRA, respectively. Furthermore, the dilute acid treatment is used afterward to recover the valuable Li and Co from the flashed anode wastes (FAW), leading to an overall increase in metal recovery efficiency for regenerated anodes.

Metal-ion leaching tests reveal the amount of remaining inorganic oxides is ~3.7%, ~4.5%, and ~0.5% for AW, FAW, and CRAW, respectively, after removing the organic impurities. A PerkinElmer Optima 8300 ICP-OES system is used to quantify the different metal contents in the reactant and flash products and their degrees of recovery and excess yields. The concentrations of Li, Co, and Ni in the FRAW are similar to AW but ~13 times higher than in CRAW. The direct evaporation of transitional metals during high-temperature calcination leads to low concentration but their condensation at downstream causes corrosion to respective equipment. This is found to be consistent with TGA results **(Fig. 1)**. Compared to AW, the average metal recovery efficiency using a dilute HCl solution is 11% higher for FRAW due to the FJH treatment. The ultrafast electrothermal process decomposes the complex organic matrix with transitional metals into simple inorganic compounds with lower valence states, as confirmed by the XRD analysis and HRTEM images with corresponding elemental mapping results. An incomplete dissolution of SEI and other impurities during dilute acid treatment leads to a minor decrease in FRM's leaching efficiency compared to the traditional hydrometallurgical methods. Overall, the metal leaching tests show that AW from spent batteries can be an option to recycle battery materials.

XRD analysis of the untreated AW shows preservation of the graphitic structure but with an accumulation of LiF and Li_2CO_3. A small downshift of the (002) diffraction peak is observed for both FRA and CRA, indicating an increase of ~0.3% and ~0.2% interlayer spacing compared to commercial graphite (CG) anode. This indicates that the degree of purification for the graphite particles in both FRA and CRA is very close to that of CG. Deconvolution of XPS spectra reveals the C content in untreated AW is 41.8%, which rapidly increases for FRA, CRA and CG to 90.8%, 92.8% and 98% respectively. UV–vis spectra show a broad absorption peak centered at ~220 nm indicating the presence of SEI layer and the electrolyte residue in untread AW. No absorption peaks are observed for FRA and CRA when dispersed in the deionized water at a concentration of ~5 mg mL^{-1}. The D/G and 2D/G ratios representing the defects and quality of graphite are found as 0.14 and 0.56 for FRA, 0.29 and 0.44 for CRA, and 0.12 and 0.57 for CG, respectively. This confirms that FRA preserves the bulk graphitic structure and quality better than CRA. This is further complemented by the SEM images, which show graphite microparticles bound by an organic binder in untreated AW, but individual graphite microparticles in FRA after the binder's thermal decomposition. HRTEM images of untreated AW show the presence of an amorphous SEI layer outside the graphite microparticles with several embedded small Li_2CO_3 crystals, whereas FRM graphitizes the carbon content after decomposing the SEI layer and reduces the average layer thickness from ~145 to ~40 nm. Although these embedded nanoparticles are trapped by the re-formed carbon layer, they can be easily rinsed with a significantly more diluted acid solution than used in typical AW recycling.

Figure 2 shows how FRA hinders the accumulation of SEI and surface amorphization to stop the anode failure. The decomposition of SEI, organic binder, and electrolyte residue reduces ~81% and ~89% bulk resistivity for FRA and CRA, respectively, as compared to untreated AW. FRA shows improved charge-specific capacity, capacity contribution, average Li^+ diffusion coefficients, and a large surface area with several micropores leading to a slightly larger initial specific capacity and lower CE than untreated AW **(Fig. 2a-b)**. CRA shows an average specific capacity similar to FRA at low rates (<0.5 C) but it diminishes significantly at high rates. – The same is true for an increase in overpotential at high rates **(Fig. 2c-d)**. CRA suffers a faster decay (~17% after 100 cycles) during electrochemical cycling compared to FRA, which maintains a recovered specific capacity of 351 $mAhg^{-1}$ at 0.2 C and 335.9 $mAhg^{-1}$ after 100 cycles, very sim-

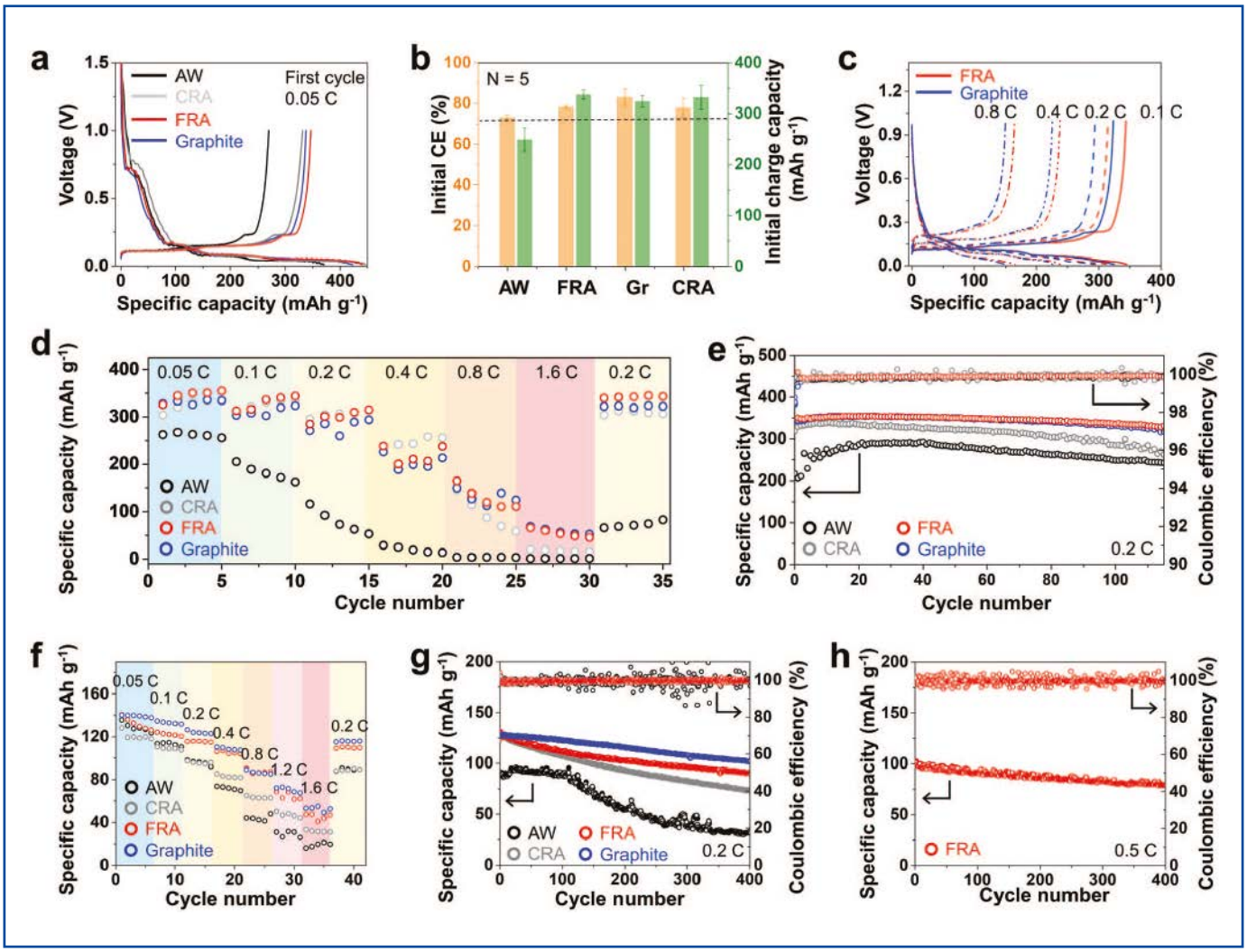

ilar to CG **(Fig. 2e)**. The stability of bulk structure and the graphene shell formation at the FRA surface contribute to its good electrochemical stability. These half-cell test results are further verified during full battery tests with $LiFePO_4$ cathodes showing an improved rate performance for FRA. The specific capacities for untreated AW, FRA and CRA are found as ~94.9, ~131.1, and ~129.8 $mAhg^{-1}$, respectively, **(Fig. 2f)**. FRA shows ~77.3% capacity retention after cycling at 0.5 C for 400 cycles **(Fig. 2h)** and better electrochemical stability with 0.078% decay per cycle as compared to 0.11% and 0.055% for CRA and CG respectively **(Fig. 2g)**.

GREET 2020 and Everbatt 2020 are used to calculate the LCA of FRA considering economic and environmental impacts from the origin of the reactants to the production of 1 kg battery-grade graphite at the factory (except the disposal) for four different methods – (A) synthetic graphite prepared from hard coal and crude oil, (B) CRA prepared from high-temperature calcination method, (C) FRA from FRM, and (D) natural graphite from mined ore. The LCA analysis shows substantial reductions in recycling cost, greenhouse gas emissions, and water and energy consumption for FRA as compared to the rest (~85-98%, ~39-51%, and ~60-81% reductions than methods A, B and D respectively). This huge reduction is credited to FRM's ultrafast electrothermal reactions, which thermally decompose and remove the resistive impurities gathered on the spent anode and thereby significantly increasing the overall energy efficiency.

Figure 2. The electrochemical performance of flash-recycled anodes. a) First cycle voltage profile of AW (black), CRA (gray), FRA (red) and commercial graphite (blue) at 0.05C. The areal capacity is ≈2.0 mAh cm^{-2}

Digest of
Chen W, Salvatierra R, Li J, et al.
Flash Recycling of Graphite Anodes.
Adv. Mater. 2023, 35, 2207303.

A Comprehensive Understanding of the Aging Effects of Extreme Fast Charging on High Ni NMC Cathode

Adapted from Tanim *et al.* (2022)

Cathode degradation issues (i.e., cracking and surface degradation) during extremely fast charging (XFC, 10-15 min battery charging time) of electric vehicles is a less researched area when compared to the well-explored Li-plating problems at the anode. For low loading, cathode degradation is less concerning during early cycles but becomes severe under moderate loading, which cannot be properly captured by typical coin cell studies. This is true for low Ni-containing MNCs, such as graphite/NMC532 single-layer pouch cells (SLPCs), graphite/NMC622, or NMC532 cells. Particularly the aging issue for NMC532 remains minimal in early cycling but becomes dominant in the later cycles for >90% charge acceptance. The separation of the inter-primary particles (IPP) within the secondary particles (i.e., cracking) and minor surface reconstruction are understood as the main reasons for degradation. The continuum-level damage models predict that the Li-gradients induce higher surface-level lattice strain leading to degradation at a higher C-rate, which is highly influenced by the secondary particle size, morphology, grain size, and orientation. In this work, a low Co-content cathode candidate NMC811 has been chosen for its potential (i.e., higher specific energy, ionic diffusion, and conductivity) in high-energy-density Li-ion battery applications. The research on NMC811's benefits is scarce and without any comprehensive understanding of the degradation modes, failures, and cycle-life implications. Thus, a wide-ranging study has been undertaken to explore the performance of graphite/NMC811 SLPCs at different fast charging rates (1C-9C) and the state of charge (SOC, 35-100%). The IPP architecture has been characterized by SEM-EBSD and two different modeling tools (such as pseudo-2D and 3D continuum-damage models) are used to predict NMC811's performance and aging as compared to NMC532.

Table 1 shows the cell designing parameters and the testing conditions for several graphite/NMC811 SLPCs, which are tested for fast-charge cycle-life evaluation at different CC-CV fast charging rates and voltage-constrained conditions at the most aggressive 9C rate. Post-testing analysis has been carried out at 450 and 600 cycles for max 4.1V cells (~100% SOC) and at 1000 cycles for 9C- low-voltage condition cells. The material characterization is performed using SEM-EBSD, HRTEM, EELS, and inductively coupled plasma mass spectroscopy (ICP-MS) using a Perkin Elmer NexION 2000. The P2D model is used to compare the design modification requirement for NMC532 and NMC811 with the same areal loading. The continuum-damage model is used to analyze

Table 1. Cell design parameters and testing conditions.

Parameter	Anode	Cathode
Material and Composition	Superior Graphite SLC 1506T 91.83 wt% (Timcal C45 carbon 2 wt%, Kureha 9300 PVDF binder 6 wt%, Oxalic acid 0.17 wt%)	Targray NMC811 90% wt% (Timcal C45 carbon 5 wt%, Solvay 5130 PVDF 5 wt%)
Single-side Thickness with Foil, µm	57	53
Foil Thickness, µm	10	20
Porosity, %	37.4	32.8
Single-side Coating Loading, mg cm^{-2}	6.38	9.08
Electrolyte	1.2 M $LiPF_6$ in a 3:7 by weight EC: EMC, 4.2x pore volume.	
Separator	Celgard 2320	
Testing Temperature, °C	30 °C	
Operating Voltage V_{min}-V_{max}, V	3.0-4.1	
Formation Protocol	i) Tap charge to 1.5 V and hold for 15 min. ii) Rest at open circuit voltage (OCV) for 12 h. iii) 3 cycles at C/10. iv) 3 cycles at C/2. v) Hold at 3.5 V (≈20% SOC) for 6 h.	
N:P Ratio	≈1.2 at C/10	

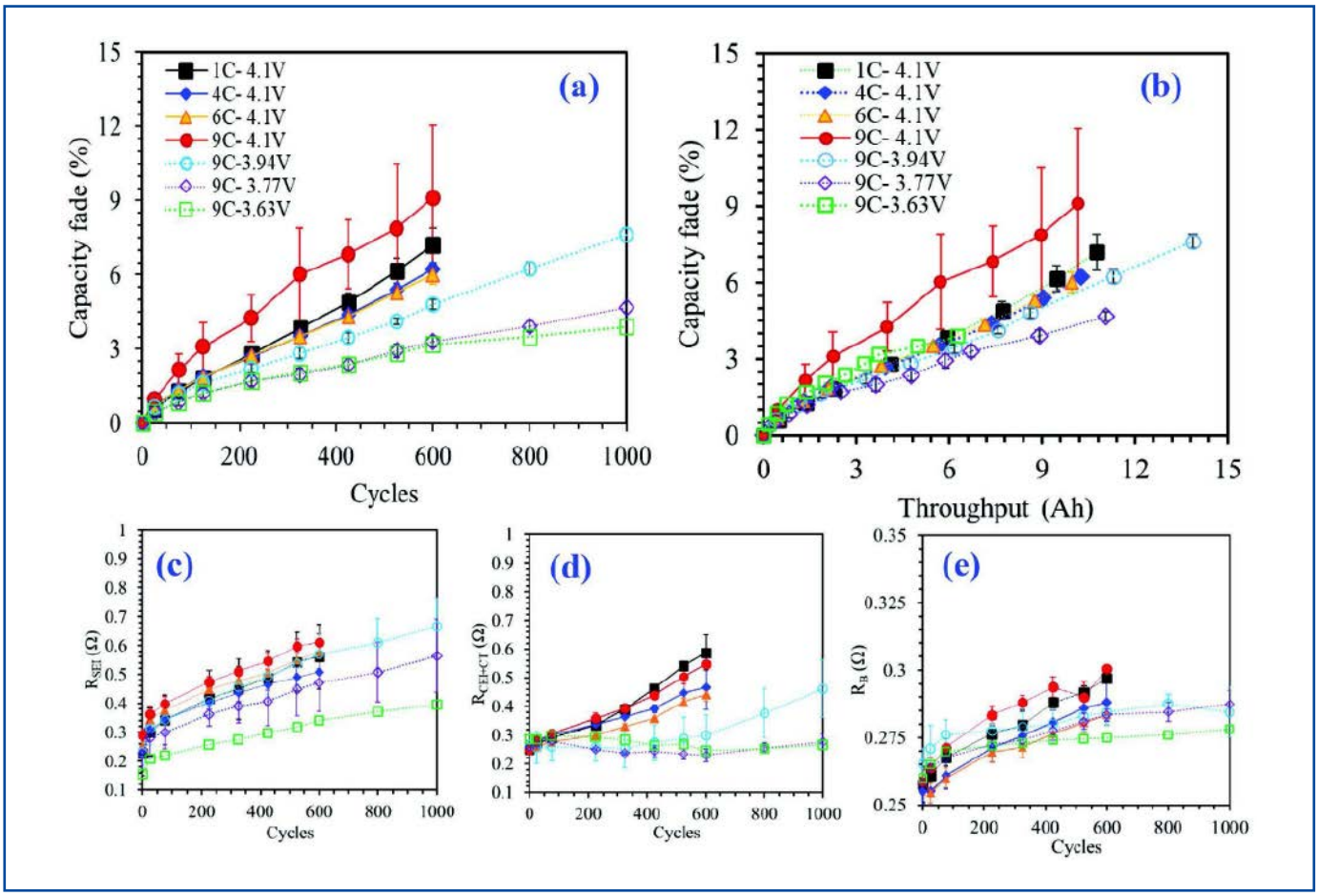

Figure 1. Cycle life cell aging performance under different XFC for Gr/NMC811 cells: a) Cell capacity fade at C/20 with respect to cycles; b) cell capacity fade with respect to cycle-by-cycle cumulative charge Ah throughput; c) SEI impedance R_{SEI}

NMC811's post-test particle level performance without considering electrolyte penetration or particle surface changes.

When compared to NMC532 cells, the experimental and pseudo-2D-modeled polarization results of NMC811 cells indicate higher impedance polarization (ohmic and charge-transfer impedances) with increased charging rate and reduced transport polarization (Li^+ transport-related losses in liquid and solid phases) attributing towards thinner electrodes, improved conductivity, and better solid-phase transport properties. Particularly, NMC811 shows 1.8× and 2× higher currents for 4C-9C transport polarization and a better total charge acceptance (99.6%-93.6% between 1C-9C) than NMC53. This is mostly credited to NMC811's improved material properties and polarization behavior rather than its thinner electrode design. When considering the capacity fade percentage of NMC811 cells for different fast charging conditions, the 9C-4.1V condition displays the highest fade with distinct variability, followed by 1C-6C conditions, with all of them showing a lower capacity fade (0.5-2.65%) than NMC532 cells **(Fig. 1 a,b)**. The same trend is closely followed by SEI and bulk impedance parameters till 600 cycles **(Fig. 1c,e)**. However, lumped CEI and charge-transfer impedance are able to capture NMC811's gradual aging issues compared to NMC532 **(Fig. 1d)**. NMC811's lower impedance leads to a distinctly better impedance behavior and therefore better aging than the NMC532 coin cell. Irrespective of C-rates, the capacity fade of NMC811 coin cells is between 2-9% and 5.1-6.8% after 425 and 600 cycles, respectively, for 4.1V condition. Particularly for the 9C-low-voltage conditions, the slow aging effect is observed even after 1000 cycles. When capacity fade is compared between NMC811 and NMC532

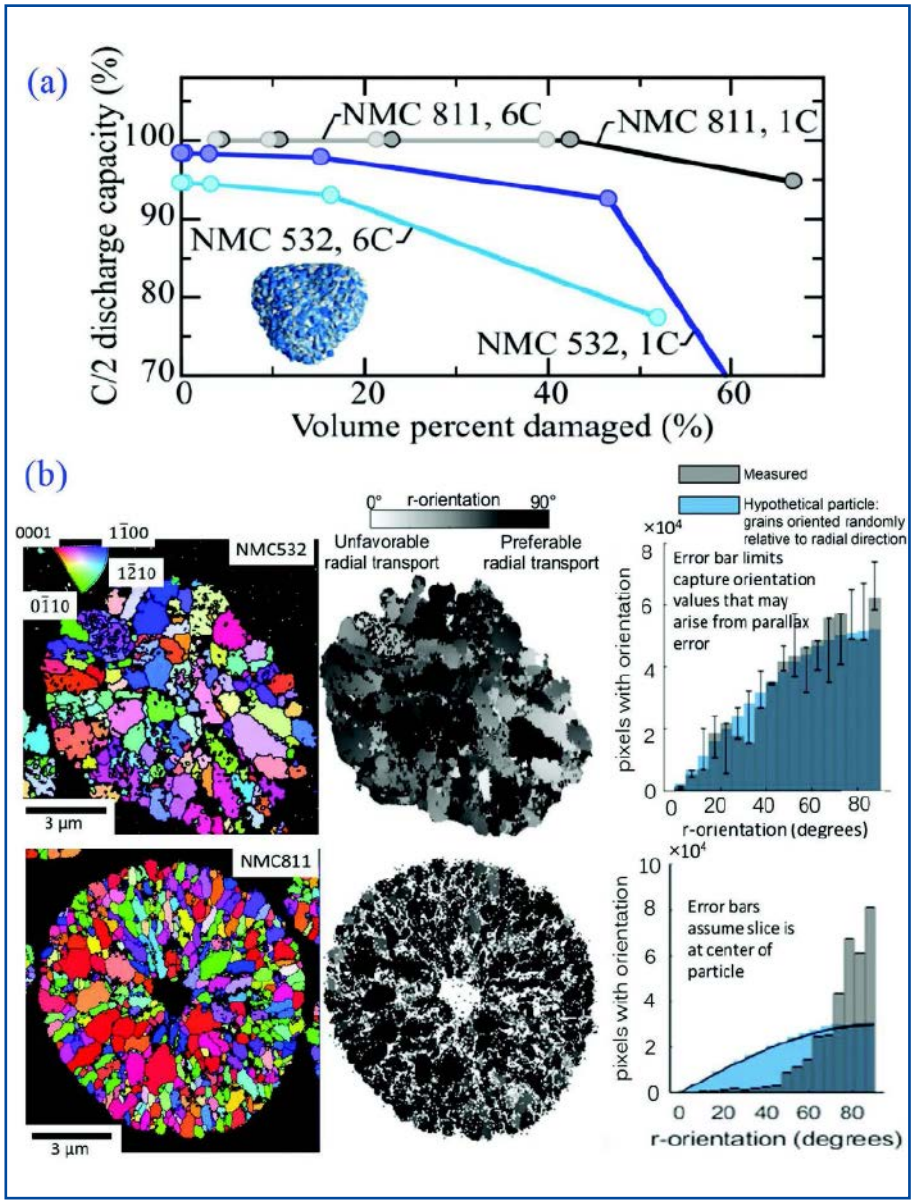

Figure 2. a) Model results showing C/2 discharge capacity with respect to percent volume damaged. Illustrated are the responses for the NMC811 particles and the NMC532 particles, respectively, after 1C and 6C charging. b) EBSD data from cross-sectioned NMC532 (top) and NMC811 (bottom) particles showing (left) the angles of grains, (middle) the angle between the C-axis of NMC and the radial direction of each grain, and (right) the distribution of those angles in grey relative to a simulated random case in semi-transparent blue. The EBSD slices are assumed to be at the center of the particles. Error bars for the NMC532 particle are the same calculation but for if the slice was for particles were sized at d10 and d90 particle diameters, i.e., that may accrue from parallax error as described in ref. [28]. Due to the characteristic void at the center of the NMC811 particle, it is assumed that the slice is at or near the particle center.

coin cells after 600 cycles for 4C and 6C conditions, the results are observed as 5-7% and 21-24%, respectively. ICP-MS confirms that the Li-ion loss (also identified by the isolated Li-plating spots) is bigger for NMC532 than for NMC811 at similar cycling conditions, which dominates the capacity fade. The material loss from the cathode becomes a silent aging mode, evidenced by the migration of transition metals from NMC811 to the anode as Co>Mn>Ni irrespective of the C-rate.

SEM images of NMC811's cross-section show IPP grain boundaries in every particle, with cracking in the larger ones after 425 cycles, which is aggravated more after 600 cycles, irrespective of C-rates. The SEM images of 9C-low-voltage-1000 cycles conditions confirm that the particle damage is simultaneously influenced by the initial charging rates, upper cut-off or average voltage, and cycle numbers. The surface degradation is characterized by the formation and thickness of the surface reconstruction layer. The regions undergoing dynamic Li transport lead to severe reconstruction. The HRTEM images and corresponding EELS line scans show that the reconstruction layer of NMC811 particles has a rock-salt structure at the outermost surface, which is bridged with a mixed atomic layers structure. The bulk

material retains the layered structure after cycling, except for the 9C-low-voltage-1000 cycles conditions, which experience the formation of nano-voids due to oxygen release and reduction of Ni-ions at the surface. It should be noted that the same role is played by Mn for NMC532 but has the most negligible effect for NMC811. The thickness of the surface reconstruction layer is found to be dependent on both the C-rates and voltages, similar to the CEI layer thickness. When Li diffusion channels are perpendicular to the Li^+ diffusion pathways, the degradation becomes less severe, and no disorder layers are visible.

Figure 2 shows the 3D reconstructed particles' secondary responses via continuum-damage modeling. The same particle geometry and random grain orientations are used for NMC532 and NMC81. Less capacity is reached for higher damage percentage and high C-rate for the NMC532 particles, whereas NMC811 particles maintain almost 100% capacity even at high damage percentage **(Fig. 2a)**, attributing towards its high solid-phase Li-diffusion coefficient, better conductivity due to high Ni-content, and significantly lower impedance growth. The r-orientation (angle between the radial line and NMC's c- axis) distribution plots indicate a faster Li-transportation into the particle for more radially aligned grains. NMC811 grains demonstrate a strong preference towards radial alignment, whereas random orientation is observed for NMC532 grains **(Fig. 2b)**. Besides this, the radial alignment leads to less ionic isolation between grains, which in turn hinders the radially-directed cracking.

The lost charge-acceptance due to capacity fade quantifies the aging in a way where NMC811 shows lower charge-acceptance loss than NMC532 in comparable conditions irrespective of C-rates. Decreasing the charge cut-off also reduces the charge-acceptance loss and therefore aging. At lower C-rates, cracking becomes the dominant aging mechanism for NMC811, but both surface and interphase degradation speed up the aging at higher C-rates. NMC811 experiences more material degradation and less cracking than NMC532, indicating that aging is more sensitive towards cracking. The strong radial alignment of NMC811 grains can also influence cracking tendencies. Advanced surface protection and crack mitigation tactics can be implemented to further improve NMC811's performance, but the latter is expected to be more effective. Overall, NMC811 is a better candidate than NMC532 to enable XFC in Li-battery applications.

Digest of
Tanim T, Yang Z, Finegan D, et al.
A Comprehensive Understanding of the Aging Effects of Extreme Fast Charging on High Ni NMC Cathode.
Adv. Energy Mater. 2022, 12, 2103712.

Overcoming Lithium-Ion Battery Obstacles for the Alternative Energy Revolution

Global climate initiatives, in conjunction with an increase demand for battery reliant technological innovations, are driving the alternative energy revolution. Rapidly emerging as a cornerstone technology in this revolution are lithium-ion batteries (LIBs). Libs are providing key energy advantages to enable innovations in the energy, automotive and tech sectors.

LIBs made their debut in consumer electronics in 1991, with a bulky design and limited energy capacity. Since then, LIBs have evolved a more compact design and greater energy storage. Energy storage is described as energy density, the total energy divided by the batteries' weight or volume. By increasing energy density, LIB manufacturers could produce smaller batteries with greater energy capacities. Energy density is one reason lithium is so attractive, the third element of the periodic table is super lightweight, delivering a lot of energy in a small package. In addition to their high energy densities, LIBs have long lifetimes and low toxicity, positioning themselves as one of the dominant battery technologies.

However, there are two major obstacles that the LIB industry is facing that need to be overcome to stay dominant: raw material acquisition and battery failure prevention. As the LIB industry increases with growing demand, added pressures will be placed on procurement of key raw materials. Specifically, the demand for lithium, cobalt, and graphite is projected to increase significantly in the coming decades. Procurement of raw materials for LIBs have a variety of environmental and social considerations that need to be addressed to ensure ethical development practices.

The LIB industry must also tackle the issues that drive LIB failure and thermal runaway. While most lithium battery failures are small, isolated incidents, there have also been large scale accidents. Such battery failures have led to explosions and fires, resulting in significant damage and deaths. Fortunately, there are now resources and advances designed to prevent battery failure and thermal runaway. In this white paper, we shall investigate the issues surrounding raw material procurement and battery failure, with an emphasis on the newest innovations and technologies to solve them.

LIB Raw Materials

LIBs normally consist of a separator, electrolyte, negative electrode (commonly graphite), and positive electrode (typically layered lithium transition metal oxides i.e. cobalt, nickel, and manganese), see Figure 1. The separator, acting as electronic insulation, is saturated with an electrolyte (i.e. lithium hexafluorophosphate), which is dissolved in organic carbonate solvents.

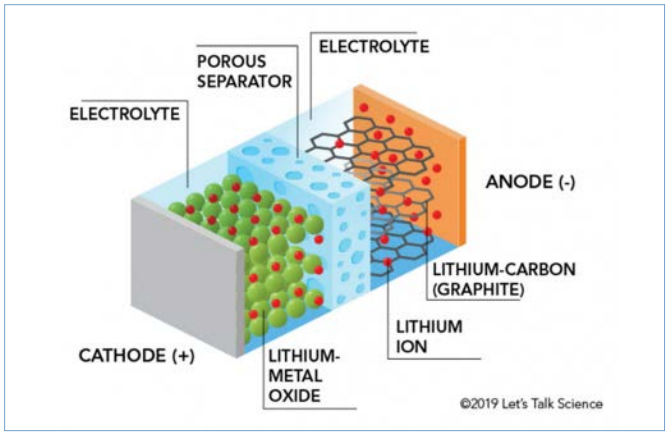

Figure 1: General Anatomy of a Lithium-Ion Battery.

The raw material extraction of these metals relies on an expanding mining industry and high purity metal processing that will continue to increase complexity of processing techniques for the future. The primary mechanisms that are driving the evolution of mining's technological innovations are safety considerations and operational benefits.

Safety

Exposure to high levels of metal particulates found in dust during extraction and other high-risk operational tasks has pushed the mining industry to replace laborers with remote-controlled and autonomous robotic equipment. Remote-controlled and autonomous robotic equipment has led to enhanced exploration of flooded mines and deep-sea deposits. Additionally, the COVID-19 pandemic has revealed that remote-controlled and autonomous robotic equipment can help manage COVID-19 risk, and risk of future pandemics, by mitigating close contact situations during operation.

Technological innovations including remote operations, robotics and automation are transforming mineral extraction industry into what is being referred to as Industry 4.0, see Figure 2. The increase in digitally connected and integrated systems has enabled a variety of new technology developments such as the internet of things and advanced analytics. These technological innovations are primed to optimize the industry by providing operators better analytical tools to make better decisions and improve production efficiency.[1]

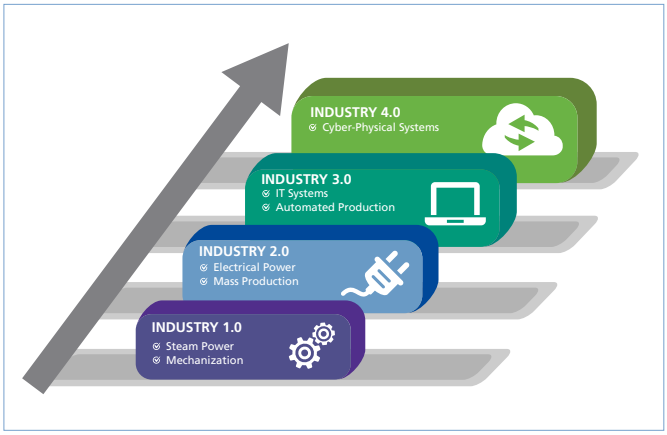

Figure 2: Industrial Revolutions.

Environmental Impact of LIBs

Lithium battery innovations continue to set a gold standard for, and reinforce the promise of, more efficient battery systems. However, even though LIBs may hold the potential to push green energy solutions into ubiquity, paradoxically, one of the biggest hinderances to LIB's expanded development is the cost raw materials acquisition places on the environment.

LIB cells are primarily responsible for the energy and carbon footprint in the production of lithium batteries. 40% of the total climate impact of LIBs is due to the mining, conversion and refining of the active materials of the cell.[2] The cell production is the second most energy consuming process with 20% total CO2/kWh.[2] In order to mitigate the environmental impact of LIBs several innovative processes are being developed.

Environmental Solutions for LIB Development

Geothermal Powered Lithium Extraction

Vulcan Energy has developed their Zero Carbon Lithium™ extraction technique utilizing geothermal power. As part of the EU's climate agenda, Vulcan aims to produce lithium for 1 million batteries per year. Their production is set for the beginning of 2024 and will significantly develop the EU's ability to produce its own domestic car batteries.

Subsurface Brine Extraction for High Purity Lithium

Lithium salts, lithium carbonate or lithium hydroxide monohydrate, have the current standard of 99.5% pure. However, there is an increased market for high purity lithium that delivers a 99.99% pure product. Higher purity lithium salts ensure battery performance and remove the risk of impurities, such as sodium, that can lead to battery failure and overheating.

Prairie Lithium has developed an unconventional Li approach using Li enriched brine reserves in western Canada. Their method utilizes subsurface brines that contain 15-300 ppm

Lithium, which is significantly more enriched than conventional seawater at 0.2 ppm Li.[3] The Li brines are analyzed using atomic absorption (AA), an effective test to find higher metal impurities, and inductively coupled plasma (ICP) testing, used to evaluate range and concentration of metal impurities. Once the brine location is established, it is surfaced for the DLE process where Li is removed from the brine. Finally, the lithium concentrate is converted to battery grade LiX.[3]

A cornerstone technology for the determination of impurities in high-purity metal raw materials is ICP-OES. PerkinElmer Avio 550 ICP-OES possesses the required sensitivity to perform high purity analyses, making it an excellent option for high-purity lithium extraction. Additionally, its sample introduction systems are resistant to high salt matrices and highly corrosive samples. Table 1 shows various analytes identified in high-purity lithium carbonate raw materials used in LIB production.

Table 1: Analytes in High-Purity Raw Materials Used in Li-Battery Production-Lithium Carbonate.

Analyte	Lithium Carbonate (mg/kg)
Al	0.76
Ca	79.5
Cr	0.082
Cu	0.295
Fe	3.86
K	228
Mg	35.5
Mn	0.36
Na	480
Pb	2.75
Zn	2.70

Recycling LIBs

It is estimated that nearly 11 million tons of previously used LIBs will exist by 2030.[4] Currently, there is not an adequate framework to handle this excess waste. Recycling LIBs is going to be instrumental in ensuring an adequate supply of raw materials while mitigating damage to the environment.

The process of recycling LIBs starts with deactivating and shredding of the old battery module, which is discharged and dismantled. The dismantling of the module happens under inert atmospheric conditions to avoid thermal runaway. Volatile electrolyte residues are removed, and hydrometallurgical procedures are carried out using pH dependent precipitation of salts to recover materials like lithium and cobalt. Characterization of LIB materials using elemental analysis and cell chemistry are paramount in order ensure effective recycling efficiencies.[5]

Repurposing LIBs

Repurposing of these spent batteries is another strategy to reduce the toxic waste and pollution burden associated with this projected LIB expansion. After an electric vehicle battery drops below 70-80%, they lose the ability to power the car.[6] However, they retain enough capacity for other functions requiring stationary storage such as household and industrial power applications. Currently, the primary limitations of repurposing LIBs are the lack of data-sharing to support the residual value of battery capacity, battery standards, and limited clarity regarding liability.[6]

Battery Failure

There are several abuse factors that can lead to battery failure, but the most common to consider are overcharging, battery misuse, overheating, manufacturing defects and short circuits caused by dendrites. Any of these abuse factors can lead to thermal runaway, as it is created in a battery when the rate of internal heat generation exceeds the rate of heat that can be expelled.[7]

Overcharging can create a chemical reaction between the electrode and electrolyte, initiating the transition of the liquid electrolyte into a gas. Overheating also causes this liquid electrolyte to transition to a gaseous state. As the gas builds, pressure increases beyond what is able to vent. Once the separator is compromised by this pressure, chemical interactions between the cathode and anode lead to a short circuit and thermal runaway.

Thermal Runaway

Thermal runaway begins after the cell has been compromised and starts a chain reaction that produces significant amounts of trapped thermal energy. During the process of thermal runaway, the battery can heat up from room temperature to nearly 700°C in a matter of seconds. The heat degrades the electrolyte into flammable and toxic gases, while the cathode begins to decompose releasing oxygen, accelerating the thermal runaway chain reaction. Once the flammable gases react with oxygen and heat, a combustion reaction is created. The risk of explosion during thermal runaway increases as the pressure continues to build in the battery cell. Thermal runaway is an exothermic reaction and once it starts it will generate its own oxygen, making it very difficult to extinguish.[8]

There have been numerous incidents of thermal runaway in LIBs that have led to the destruction of electric vehicles, cell phones, laptops, and even whole industrial energy facilities. The reason why every smart phone doesn't turn into a fire hazard while charging overnight is due to the battery management system (BMS). LIBs utilize the BMS to manage charge and discharge controlling, faulty diagnosis, parameter detection

(total voltage, numeric temperature, total current), balance control, and thermal management.[9]

Even though the BMS is designed to mitigate thermal runaway risk, it occasionally fails at managing one of these parameters due to manufacturing defects in the BMS (also the battery) or an abuse factor. It is vital that the proper quality and development strategies are applied to LIBs, and their associated components, along with the utilization of off-gassing technologies to provide robust thermal runaway prevention.

Preventing Thermal Runaway

With the initiation of an abuse factor, thermal runaway can lead to destroyed equipment and dangerous meltdowns. Prevention of thermal runaway can be conducted at several points during development of the LIB and throughout the lifetime of the LIB in the field. During development careful analytical analysis of the separator, electrolyte and binder can prevent the formation of impurities and provide vital information on material compositions to support thermal runaway prevention. Post-production, detection of off-gassing compounds in the battery using TG-IR-GCMS and thermal runaway sensors, provides LIB operators fail safes to prevent thermal runaway before it starts.

Separator Analysis

Lithium battery failure is often caused by degradation of the battery separator. The synthetic polymers used in separators in the LIB industry provide both thermal and physical properties that can ensure battery integrity and prevent battery failure. Poor quality polymers, or polymer blends, utilized during manufacturing can lead to LIB failure, thus, verification and quality testing of those materials during every stage of manufacturing is necessary. Infrared (IR) spectroscopy is ideal for qualitative analysis of polymer starting materials and finished products as well as quantification of components in polymer mixtures.

Fourier transform infrared (FT-IR) spectroscopy is a rapid and non-destructive analytical technique which delivers a sort of compositional "snapshot", as the measured data is specific to covalent bonds present in the tested material. This information helps LIB manufacturers to verify they have received the correct raw materials and can also be used in a "forensic" approach, through analysis of failed components to help identify the root cause.

Degradation can occur during charging and discharging, and results in changed chemical bonds and structure, which provides insights when inspecting binder or separator materials. These analyses can be conducted in bulk, using an instrument such as the Spectrum 3 FTIR, or in microscale, using the Spotlight 200i or 400 infrared microscopes. Figure 3 shows microspectroscopic measurements of a degraded separator, acquired with a Spotlight 400 microscope equipped with an ATR imaging accessory[10].

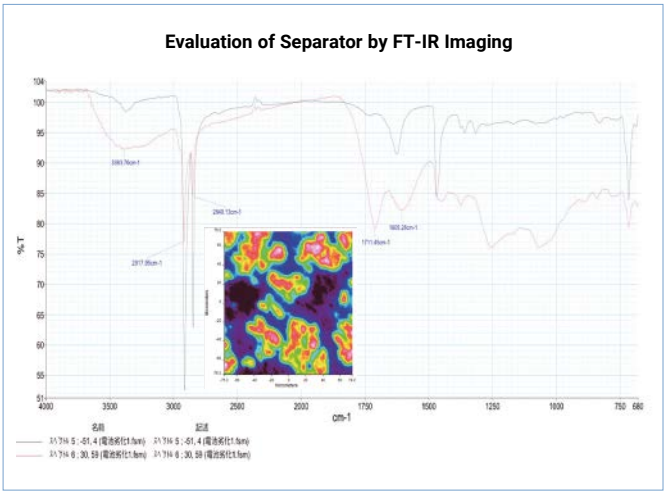

Figure 3: IEvaluation of oxidative degradation is shown here through ATR imaging of the separator.

Evaluation of separator materials can also be conducted by differential scanning calorimetry (DSC), which is used to study the melting profile, electrolyte decomposition, the enthalpy of phase transitions, thermal stabilities, and other thermal properties.[10]

Binder Analysis

Lithium battery binders are responsible for holding coating particles together and reinforcing the coating to the metal or separator membrane. Additionally, binders can aid in film formation, encourage optimal particle dispersion in the solvent and help the coating disperse to deliver a uniform slurry and discrete particles to the anode and cathode. A binder's functionality, helping to maintain LIB capacity, is dependent on their stability and it is imperative that the binder resists degradation.[11]

Thermogravimetric analysis (TGA) is an indispensable tool in determining thermal stability and the decomposition profile of materials used in lithium batteries under controlled heating conditions. In Figure 4, operators were able to generate thermogravimetric data from a sample of ethylene vinyl acetate binder on the electrodes of a LIB Using a PerkinElmer TGA 8000™ thermogravimetric analyzer.[10]

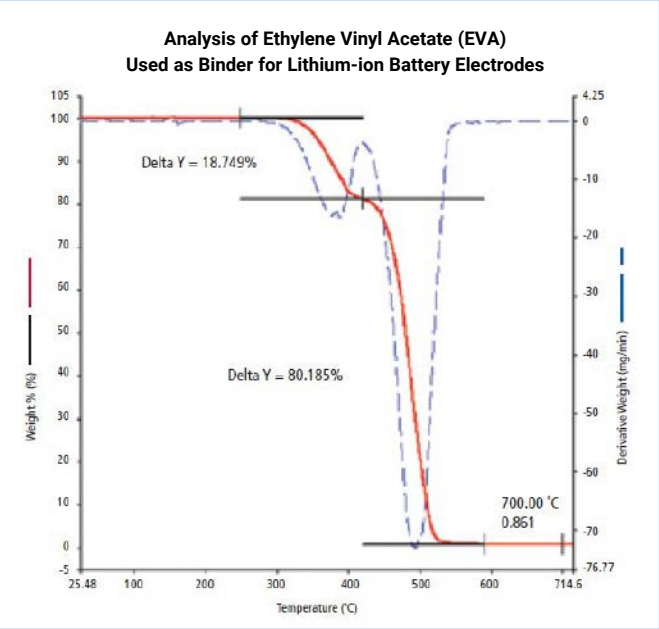

Figure 4: Thermogravimetric data generated from the analysis of EVA sample.

Electrolyte Analysis

Inductively coupled plasma optical emission spectroscopy (ICP-OES) is used for a variety of analyses in the Li battery industry and can be very useful in the analysis of impurities in LIB electrolytes. The presence of electrolyte impurities increases the risk of battery inefficiency and failure. In Table 2, the following electrolyte impurity analysis was carried out utilizing PerkinElmer's Avio® 550 ICP-OES, offering excellent insights on electrolyte composition.[10]

Table 2: Impurities in DMC Electrolyte.

Analyte	DMC Electrolyte (µg/L)
Al	2480
Ca	96.4
Cd	43.6
Fe	158
K	136
Mg	2.20
Na	3172
Pb	192

Compositional testing, such as determining the composition and ratio of cyclic carbonates, offers valuable insights into the degradation of components resulting from repeated charging and discharging in LIBs. In Table 3, users calculated method detection limits and method quantitation limits of a variety of cyclic carbonates with PerkinElmer's Clarus® SQ 8 GC/MS.[10]

Table 2: Calculated Method Detection Limits (MDL) and Method Quantitation Limits (MQL).

Analyte	MDL (µg/mL)	MQL (µg/mL)
Dimethyl Carbonate	0.111	0.444
Ethyl Methyl Carbonate	0.176	0.705
n-Propyl Propionate	0.171	0.684
Diethyl Carbonate	0.172	0.690
Vinylene Carbonate	0.166	0.664
Fluoroethylene Carbonate	0.104	0.415
Ethylene Carbonate	0.146	0.584
Propylene Carbonate	0.086	0.343
1,3-Propanesultone	0.080	0.320

Off-Gassing Monitoring and Sensors

After an abuse factor initiates off-gas generation, there is a window of time where the gas production can be detected, and strategies can be set in place to remove the abuse factor or shut the battery down entirely. It is within this window that off-gas monitoring and sensors can be instrumental to thermal runaway prevention.

Once off-gasses are detected, manual or automated processes can be implemented to shut down the battery pack and continue to monitor for smoke as a preventative action. The key question becomes which gases are important to monitor? Given that the components of LIB are constantly changing, due to the dynamic nature of material optimization, it is important to get your batteries unique off-gas signature.[12] Once established, you can determine key gasses to monitor along with their concentrations over time. Getting this off-gassing signature can help LIB manufacturers find the correct sensor or provide the necessary data to detect and design their own sensor, unique to their battery system. To detect off-gases, it is important that sensors or monitors be capable of detecting a cocktail of off-gases that are uniquely dependent on the LIB used.

Off-Gas Monitoring Technologies

Due to the wide variety of lithium salts used in the cathode of LIBs, such as lithium cobalt oxide, lithium manganese oxide, lithium nickel cobalt aluminum oxide, and lithium iron phosphate, off-gassing profiles will differ depending on the internal elements of the LIB. Volatile organic compounds are common denominators in most LIBs. Once an abuse factor initiates the battery failure process, VOCs will be released along with carbon monoxide, methane, ethane, ethylene, hydrogen chloride, hydrogen fluoride, and hydrogen.[12]

Analytical testing methods using TG-IR-GCMS are ideal technologies for a comprehensive analytical testing option of

off-gas signatures. Individual gas compounds may not provide enough of a signal prior to thermal runaway to give proper notice, so a TG-IR-GCMS method that calculates off-gas signatures together will provide robust post-monitoring sensor capabilities.

TGA analysis enables quantification of the weight loss of a material at specific temperatures. Mass spectrometry (MS) enhances the technique by providing the ability to identify the species that evolved during thermal analysis. If complex gases, such as the cocktail of off-gasses and VOCs, evolve during an event, the MS data is difficult to interpret. The use of TG-GC/MS adds chromatographic separation of co-evolved gases, enabling identification of individual components, making data interpretation easier than TG-MS.

Overcoming Obstacles

Investment in reliable equipment offers a significant ROI for those involved in LIB development. Analytical solutions that assess separators, binder, electrolytes, and other LIB components will ensure battery integrity and reduce the risk of battery failure. Safeguards in off-gassing monitoring provide additional security against thermal runaway, preventing injury, death and significant costs.

Utilizing the proper analytical instrumentation can help provide high-purity lithium and other metals for LIB development and manufacturing. These high-purity applications will yield better end products with greater battery functionality and lower failure rates.

There is no doubt that lithium battery innovations will continue to play an important role in energy, automotive and tech sectors. Overcoming the obstacles of raw material procurement and reducing battery failure are imperative for LIB manufacturers to achieve a dominant position in the alternative energy revolution.

References

1. Modern Mining Trends and Challenges. (n.d.). July 14, 2021. PerkinElmer. https://f.hubspotusercontent40.net/hubfs/547446/LabManager/Downloads/PerkinElmer/203724%20WTP%20Mining%20Trends-FINAL%20(002).pdf

2. What is the environmental impact of lithium batteries? (n.d.). Changeit.app. https://changeit.app/blog/2021-03-26-environmental-impact-of-lithium-batteries/

3. The Mining and Refining Challenges to Produce High Purity Lithium. Hanton, D. Scott. Lab Manager. July 19, 2021. https://www.labmanager.com/big-picture/lithium-ion-battery-production/the-mining-and-refining-challenges-to-produce-high-purity-lithium-26230

4. Low-Temperature Molten-Salt-Assisted Recovery of Valuable Metals from Spent Lithium-Ion Batteries. ACS Sustainable Chem. Eng. 2019, 7, 19, 16144–16150. August 26, 2019. https://doi.org/10.1021/acssuschemeng.9b03054

5. The Analytical Needs for Recycling Lithium-Ion Batteries. Nowak, Sascha. Lab Manager. July 19, 2021. https://www.labmanager.com/big-picture/lithium-ion-battery-production/the-analytical-needs-for-recycling-lithium-ion-batteries-26231

6. Feasibility of utilising second life EV batteries: Applications, lifespan, economics, environmental impact, assessment, and challenges. (2021). Alexandria Engineering Journal, 60(5), 4517–4536. https://doi.org/10.1016/j.aej.2021.03.021

ANALYTICAL SOLUTIONS TO DRIVE THE ENERGY REVOLUTION

Our comprehensive portfolio of analytical solutions for battery materials testing has the flexibility to support ongoing innovations and keep up with your laboratory's ever-changing requirements.

Carry out investigations to improve the performance, positivity, conductiveness and other properties of your battery parts such as cathode, anode, electrolyte, separators, membranes, and binders.

Providing the chemical and material analysis you need, we help you innovate in batteries for safety, performance, power, longevity, scale and weight.

Learn more at
www.perkinelmer.com/category/energy-storage

PerkinElmer®
For the Better